reaction creates heat in the forward direction, adding to the force of the eruption. The ejected material is SiO_2 and GeO_2. The escaped fluoride gases, in the presence of water, will be in equilibrium with SiO_3H_2, GeO_2 and HF; this is essentially the reverse of the reaction proceeding from the point of the protonation of the glass surface. This regenerates the HF in a catalytic manner. There are some side reactions that may slightly decrease the active HF concentration; however, the HF is recoverable for reaction with the glass until the HF is physically removed from the system. The SiO_2 precipitates as a silica gel when the water around it evaporates giving rise to spherical shapes surrounding the hole. The spheres are silica in a hydration state, but not vitreous glass. The same occurs for the GeO_2, except that it forms a shard-like crystalline structure. The reaction conserves mass and energy.

The shape of the cup in the cladding area reflects the speed at which the reaction occurs in the pure silica material and its increasing speed in the Ge rich material. A FEA model was constructed for the BF04515 fiber to understand the internal stresses in the glass with a "rocket engine" defect when the fiber is under a 25% strain (Figure 24a through c). Figure 25a through c shows that the internal stress in the fiber in this case rises by a factor of three over a section, which is experiencing the same amount of strain with no "rocket-engine" defect.

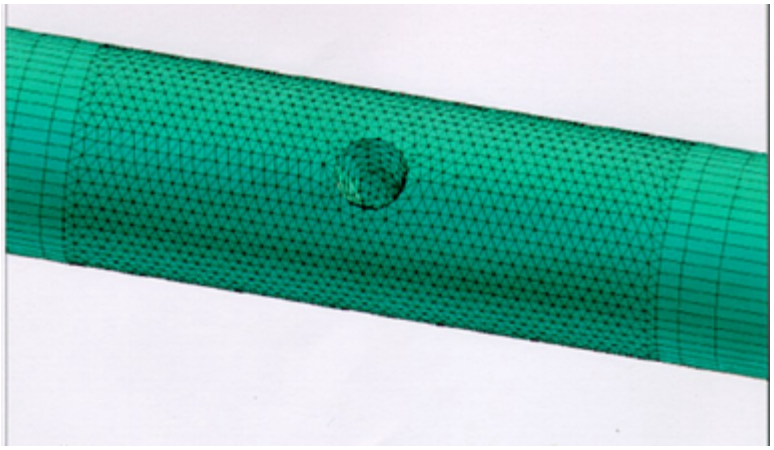

a. Element Mesh of Flawed Fiber Geometry

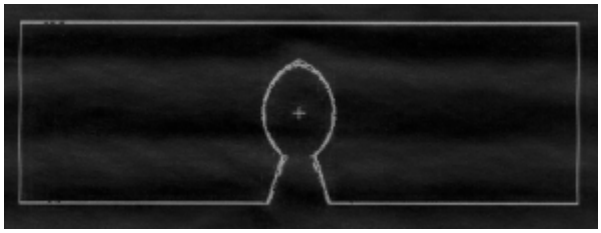

b. Side View of "Rocket Engine" Defect

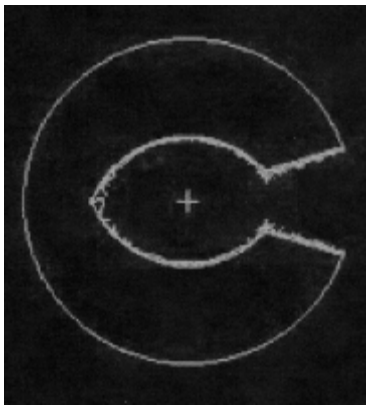

c. Crossectional View of "Rocket Engine" Defect

Figure 24 Model of "Rocket Engine" Defect

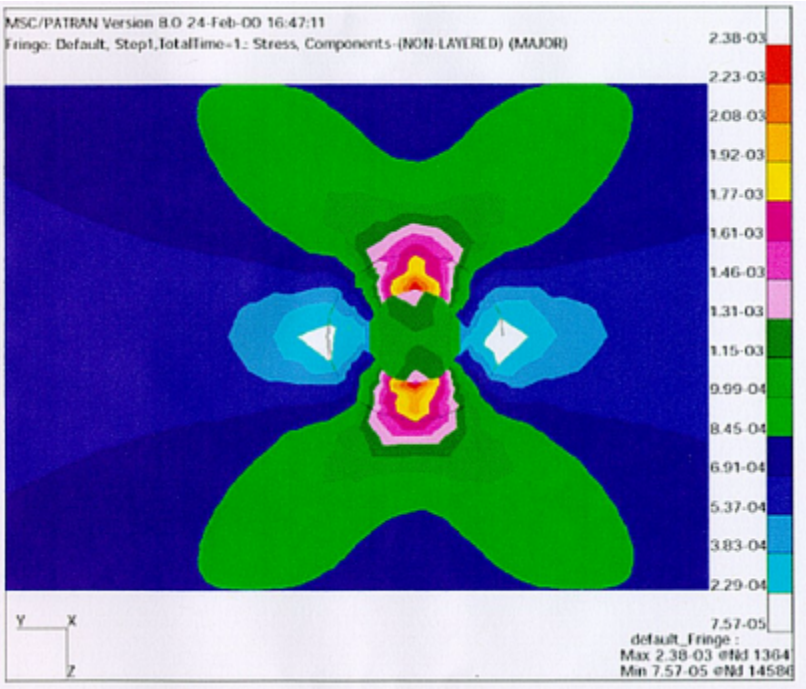

a. Stress in Flawed Fiber Under 25% Strain (view from top looking down into the hole)

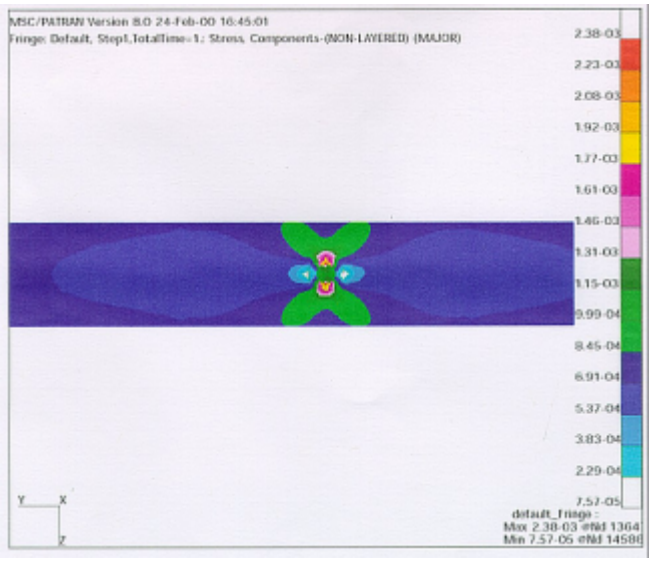

b. Top View of Stress Model

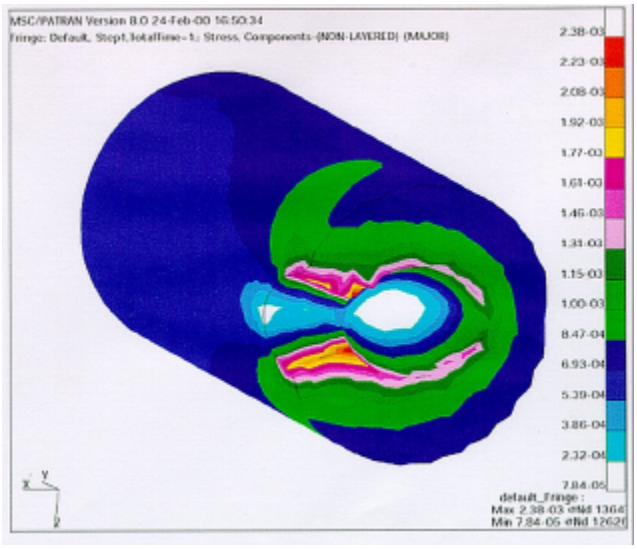

c. 45° Cutaway View of Stress Model

Figure 25 Stress Predicted by Fiber Model

Lucent Technologies experimented with BF04515 fiber from a cable with “glows”. The polyimide coating was stripped and the grounded, carbon coated fiber was exposed to a 1 kV source (wire electrode). An arc discharged through the air between the wire and the fiber. The sample was then exposed to both aqueous and vapor HF (in a humid environment) [ref-16]. HeNe light was transmitted through the fiber during the test and when light began to leak out of the side, the test was stopped. Figure 26 shows the resulting defect with the characteristic bulb pattern and ringed structure seen in the Boeing photographs (Figures 9). The sample was rinsed to drive off the highly corrosive HF, so it is not known whether there were any GeO_2 crystals or SiO_2 balls resulting from the experiment.

Lucent observed that the Ge-doped core etches considerably faster than the cladding. If the etch time is too long, then the entire core can be removed, leaving a silica tube with a pinhole in it. This indicates that the amount of HF present at the site is the limiting factor in the degree of etching.

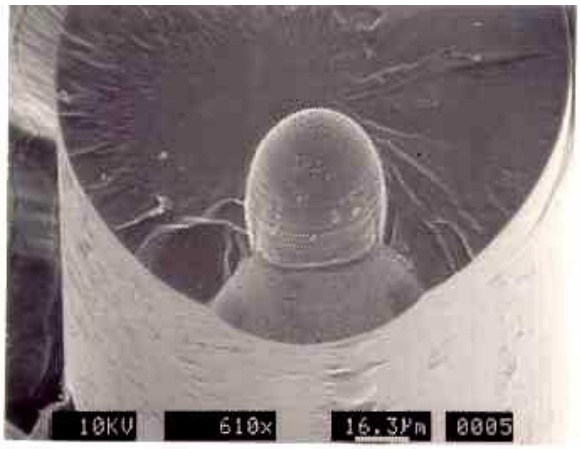

Figure 26 Etch Pit Resulting From Experimentation

Experiments were performed on 2 inch long samples of fiber removed from NFOC-2FFF-1GRP-1 cable and exposed to the vapor over liquid HF. Some of the samples had been exposed electrostatic discharge from a Tesla coil, that breached the carbon coating in small discrete points. The polyimide was removed from one half of the sample and left in place on the other half. The entire sample was exposed to HF in a liquid form for approximately 36 hours. The samples were monitored throughout the test to look for the evolution of etch pits at the induced carbon breaches. The glass was found to be etched through the pin-holes and through the endfaces of the fiber. The etching on the end without the polyimide continued into the carbon/polyimide coated section and the carbon left behind fell to the bottom of the fluid. The glass was also etched from the endface of the carbon/polyimide coated half but there was not sufficient time to allow the etch to occur past the end of the polyimide coated section. A control sample of fiber taken from OC-1260 cable with acrylic coating showed similar results in the half where the coating was left in place, however it showed a necking down of the glass from the outside in the uncoated portion of the fiber from contact with condensing HF. This showed that the carbon protects the fiber from HF attack when it is continuous.

6.4 Carbon Layer

BF04515 fiber is coated with a 25 nm coating of carbonaceous material which is intended to serve as a hermetic coating which increases the fiber’s strength and increases its reliability. Lindholm, Li et al. [ref-17] performed reliability studies with Lucent-SFT carbon coated fiber and found high strength associated with various thickness of carbon on fiber. The carbon is deposited pyrolytically as the fiber exits the draw furnace. A mixture of hydrocarbon gases enters into a chamber in the presence of a nitrogen purge. This then cracks the hydrocarbons onto the surface of the fiber. Some of the carbon species lumped into the

"amorphous carbon" group are electrically conductive and others are not. Some act as a diffusion barrier to HF and some absorb HF and act as a catalyst in etching reactions. The species of carbon, which result on the surface of the quartz cladding and their order, is not completely understood.

Breaches in the carbon coating allow the "rocket engine" defects to occur when the environment around the exposed glass contains HF. They also allow moisture corrosion of the exposed glass. Finally, when large enough, they can be located by observing light, which escapes out of the fiber through them.

During examination of the polyimide surface and the bubbles in the polyimide, a 6" sample of fiber from lot CD0588DX was believed to have a carbon breach below a prominent bubble. The polyimide was removed with sulfuric acid, which is not damaging to the carbon. Not only was a light emitting breach found below the bubble site, but companion breaches were found around it and were not associated with prominent bubble-like features. A better understanding of the molecular structure of the carbon created by Lucent-SFT's process will allow exploration of the process or handling conditions which cause breaches in it and leave the glass exposed to etchants such as water and HF. [ref-18]

6.5 Electro Static Discharge (ESD)

Respooling processes used on uncabled fiber by Lucent-SFT and BICC, are believed to expose the cable to significant levels of electrostatic charging, which when discharged, may damage the fiber coatings.
To understand the signs and magnitudes of the static charges present around the "color line" used to respool fiber at BICC, measurements were made with ESD meters (see http://misspiggy.gsfc.nasa.gov/tva/library/essays.htm for background on static charges). The values measured are presented above in Table 4. Measurements of the field strengths at several spots in the fiber draw and coating process at Lucent-SFT were similar to those measured at BICC. The respooling process at SEA was not reviewed because they do not handle uncabled BF04515 fiber.

Dupont's value for the dielectric breakdown field strength for the polyimide used by Lucent-SFT is 4 kV/mil for a 1 mil sample, at 50% relative humidity. This number will decrease at 100% and increase at 0% RH, however those values were not provided in the reference used. The thickness of the polyimide coating applied to the BF04515 fiber is 0.60 mil, thus the dielectric breakdown voltage of the coating should be at least 2.4 kV. The polymerization process used by Lucent-SFT and the presence of thinned spots at bubble sites makes it difficult to predict what level of charge will cause an ESD event terminating at the conductive carbon layer.

NASA GSFC performed a test using the set-up shown in Figure 27a to measure the breakdown strength of a sample of fiber with known flaws. The electrodes were applied between various sets of foil contacts. A breakdown strength of 2.5 kV was measured and a burn mark resulted. The burn mark was found very close to polyimide bubbles (Figure 23).

The Aerospace Corporation used the set-up shown in Figure 27b with an associated burn mark shown in Figure 22. The Aerospace Corporation found abrupt breakdown at 3.9kV in a 50% relative humidity environment, indicating a 6.5 kV/mil dielectric strength. Burn marks were found with a variety of sizes the smallest being 30 μm in diameter. They also measured the resistance of the carbon coating for lengths between 1 and 34 cm to be approximately 15 kOhm/cm, which agrees with Lucent-SFT's databook value.

a. GSFC Set-up

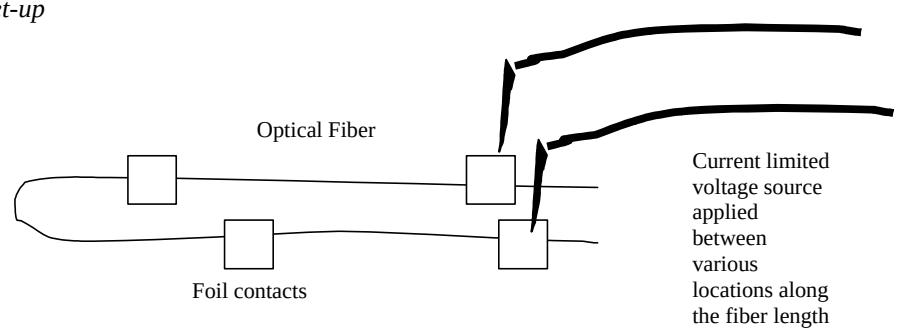

b. Aerospace Corporation Set-up

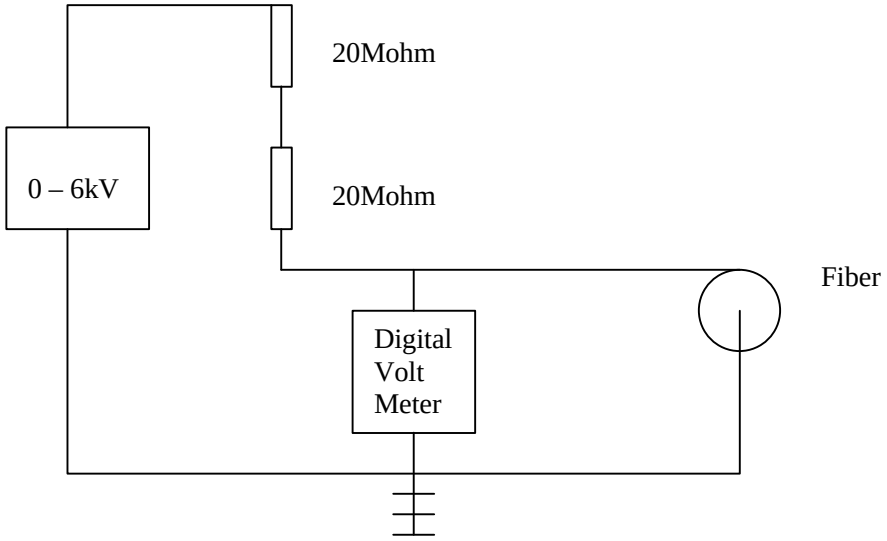

Figure 27 Experimentally Produced ESD Damage

Testing was also done with a 30 kV Tesla coil to demonstrate the conducting behavior of the NFOC-2FFF-1GRP-1 cable. When the Tesla coil tip was placed about a centimeter from the cable, the tip of the coil emitted a spark that was drawn to the cable. This spark was drawn along as the tip of the coil was moved along the cable. Upon removal of the fiber from the cable sample, the trench shown in Figure 28 was observed. Though it is not obvious in the photograph, particles believed to be polyimide surround the blackened edges of the trench suggesting that all of the polyimide did not vaporize and some of it was redeposited around the site near the trench. This demonstrated that high electric fields can cause charge travel all the way through the cable layers and damage the fiber coating.

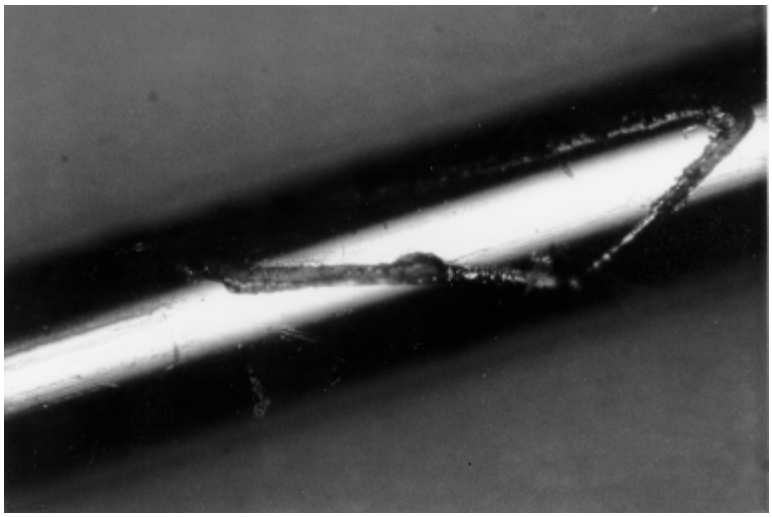

Courtesy of NASA GSFC

Figure 28 Electrical Discharge Induced Damage on Fiber Surface

Another run of this test was performed on 1996 vintage cable and the spark was found to “stick” to a particular site until the coil was move sufficiently far away and then the spark would move with the coil tip. This behavior was not investigated further. The wider portion of the trench seen in Figure 28 may be demonstrating the results of such a “sticking” behavior.

The Tesla coil test was run again using BICCGeneral’s OC1260 product, which contains an acrylate, coated fiber with no carbon layer. This cable was found to be electrically inactive. No spark was drawn from the coil even when the tip was closer than one centimeter to the cable. When the test was done with the OC1260 cable on a table, the spark went around the cable to find the grounded, conductive table.

6.6 Aeolian Motion – Vibration of Fiber Under Tension

When a steady flow of fluid passes an obstacle with a large enough speed, it is usually found that eddies are formed behind the obstacle. Such effects are familiar in the case of a stream of water "swirling" past a rock. Similar effects are also produced in a stream of air. A cylindrical obstacle, such as a rod or wire, in a stream of air sets up a double series of vortices [ref 19]. The stream of air past the wire is thus set into transverse vibrations, as alternate left- and right-handed eddies are formed and detached. This results in alternating pressure waves, which can be audible under certain circumstances. An experimental investigation of these vortex vibrations was first undertaken by Strouhal (1878) and later by Kohlrausch (1881). The frequency "f" of the tone in the air was independent of the length of the wire and also the tension of the wire, and varied only with the thickness "d" and the speed "s" of the wire through the air:

$$f = 0.185\ (s/d) \qquad (4)$$

The detachment of the alternating vortices, and the wavering of the stream of air, produces an alternating transverse force on the wire, which sets it into forced vibration at the frequency "f". We have a pronounced resonance when this frequency coincides with one of the natural modes of vibration of the stretched wire,

$$f_\eta = (n / 2*L) * \mathrm{sqrt}[T/m\mu] \qquad (5)$$

where "n" = 1, 2, 3, is the number of loops in the wire between its fixed ends, spaced a distance "L" apart, "T" is the tension of the wire, and "mu" is the mass per length of the wire. This resonance can result in a large amplitude of displacement of the wire.

The music of the Aeolian harp is produced this way. The harp consists of a number of wires of graduated thickness mounted on a sounding board. The wires are all turned to the same low fundamental note, which consequently has a wide range of overtones in the audible region. When a wind moves past these wires, and "plays" it, one or more of these wires will resonate and emit the note of the appropriate overtone. Other examples include the "singing" of overhead wires, the "sighing" and "roaring" of wind in trees, and the "whistling" of wind through tall grasses. [ref 20]

Aeolian motion may be occuring with the fiber in the draw tower. Using equations (4) and (5), one can predict the periodicity of defects which may be coincident with the resonant frequencies of the fiber in tension. The draw speed being known, we can determine that the defects spaced as shown in Figure 14 move past a fixed point at a frequency of 33 to 83 Hz.

$$T = L/S\_fib \qquad (6)$$
$$f = 1/T \qquad (7)$$

S_{fib} = Fiber Draw Speed
L = Spacial Period Between Latent Defects
T = Temporal Period Between Latent Defects
f = Frequency which the Latent Defects Pass a Point

Several aspects of the process including the glass temperature, the viscosity of the polymer in the coating cups and the speed of the capstan contribute to the tension extended to the fiber. An assumption of 4 lbs for the tension is made based on the proof test value of 5 lbs. The mass per unit length of the fiber is calculated as 42.6 mg/m. The distance between fixed points is estimated as 5 m. Equation (5) above, using these values, gives the natural vibration modes occurring at 65, 130, 195, 260 Hz and so on. Equation (4), for a fiber with a 140 to 170 μm diameter, can be used to show that an air speed of 0.7 cm/sec to 0.9 cm/sec would be required to cause the fiber to oscillate with frequencies listed above.

An experiment was done to measure the displacement amplitude for the fiber excited into motion by a shaker. A length of BF05202 (similar to BF04515 fiber was hung from a shaker, and attached to a weight of 5.96 g at its bottom. The total length that was free to vibrate was 60.0 cm. The first mode was at 30.2 Hz, the second was near 60 Hz, the third was at 90.4 Hz, and the fourth was at 120.8 Hz.

The quality factor, judged from decay times and from the full-width between half-maxima, was more than 100 for these modes. When vibrating in the fundamental mode, an amplitude of about a centimeter at the midpoint was easy to observe when the amplitude at the shaker was invisibly small (less than 0.1 mm), and the rest of the fiber was hard to see without a solid light colored background. When vibrating in higher modes, the fiber was hard to see near the "loops" but seemed to be completely stationary at its nodes: a gauge placed near a node would detect little motion. A wind directed sideways across the fiber caused it to oscillate with an amplitude of a few millimeters.

7.0 STRENGTH TESTING

Strength testing was proposed to help Boeing establish a basis for a risk assessment associated with the life of the cable already installed in the US Lab module. The findings ultimately were critically important to the understanding of the latency of the carbon breach as a defect and the prominent role of the polyimide bubbles.

7.1 Initial Testing of '96 Vintage Cable and '99 Vintage Fiber

7.1.1 Test Approach

Fiber which had not been cabled and which had been cabled were strength tested. Fiber, which had never been processed by BICC, was tested before and throughout the cabling process to understand how each step of that process affects the strength of the fiber. The testing was performed in accordance with EIA Fiber Optic Test Procedure 28, EIA-TIA-455-28B, "Method for Measuring Dynamic Tensile Strength of Optical Fiber". The set-up is shown in Figure 29. When the test was run on cabled fiber, as much of the cable was left intact as possible during the test and laser light was used to identify the locations of the breaks inside of the cable. Table 8 shows the gauge lengths and pull conditions used on the various samples. The cable and fiber that was available from which samples were selected, had already been proof tested to 141 kpsi and screened optically for the "rocket engine" defects. This provided some confidence that no large defects of that kind would factor into the strength data. For high strength samples, the breaks were expected to occur between the range of 11.2 to 12.7 lbs, based on the set-up, loading and the intrinsic strength of the fiber (> 450 kpsi). The resulting data would be plotted as a Weibull distribution which was expected to be bi-modal, one slope expected for the high strength breaks and one for the low strength breaks caused by a defect.

Table 8 Strength Testing Samples and Conditions

Uncabled Fiber Lot Number	Date of Mfr	Cabled Fiber Reel Number	Date of Mfr	Gauge Length (inches)	Pull Speed (in/min)	Effective Strain Rate (%)
CD0384X	1/21/99			20 80	0.5 2.0	2.5 2.5
CD0588X	7/22/99			80	2.0	2.5
		04055	8/1/96	80	2.0	2.5
		04056	8/1/96	20 20 20 80	0.05 0.5 5.0 2.0	0.25 2.5 25 2.5
		04162	8/1/96	20 20 20 80	0.05 0.5 5.0 2.0	0.25 2.5 25 2.5
		04165	12/19/96	20 20 80	0.5 5.0 2.0	2.5 25 2.5
		04233	12/19/96	20 20 80	0.5 5.0 2.0	2.5 25 2.5
		04240	12/19/96	80	2.0	2.5
		04244	12/19/96	20 20 20 80	0.05 0.5 5.0 2.0	0.25 2.5 25 2.5
		04245	12/19/96	20 20 20 80	0.05 0.5 5.0 2.0	0.25 2.5 25 2.5
		04250	12/19/96	80	2.0	2.5

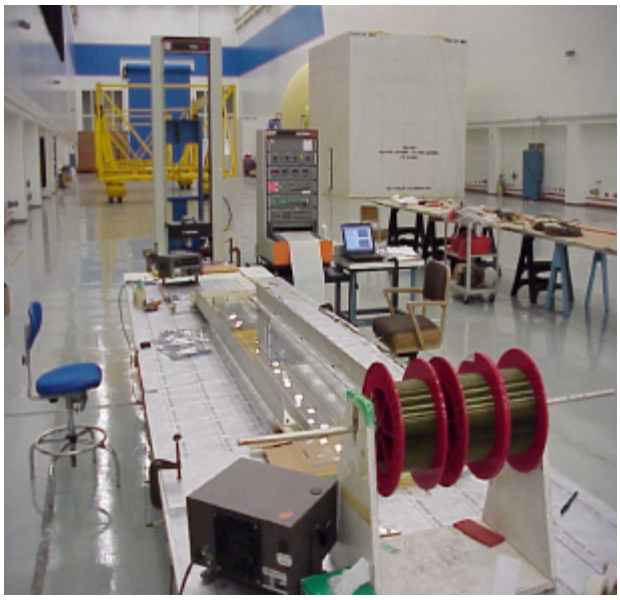

Courtesy of The Boeing Corporation

Figure 29 Test Set-up

7.1.2.1 Results: Initial Tests on Cabled Fiber

The results of the initial strength tests are shown in the Weibull plots in Figures 30 and 31. Prior analysis showed that the fiber shipped by Lucent-SFT was proof tested to 141 kpsi (@ 3.36 lbs). The cable specification requirement is for a fiber strength of 200 kpsi (@ 4.76 lbs). Lindholm, et. al., report strengths of 500 kpsi (11.90 lbs) and higher for four carbon coated fibers they have manufactured. The plots showed the high strength of the cabled fiber to be around 252 kpsi (6 lbs) and the low strength to go as low as 126 kpsi (3 lbs).

The inspections found that defects were present in large numbers that were either small etch pits at the surface of the cladding or corrosion sites in the same location. The knees in the Weibull plots, an associated slopes, show that there is more than one dominant failure mode. According to the physics of glass, the order of the curves should show the black circles (highest strain rate) located to the right of the other curves, not to the left. Figure 31 shows that the distribution of low strength breaks among the reels was significantly different even for reels with the same date of manufacture. These distributions could not be used to quantify the expected life of the cable using classical methods.

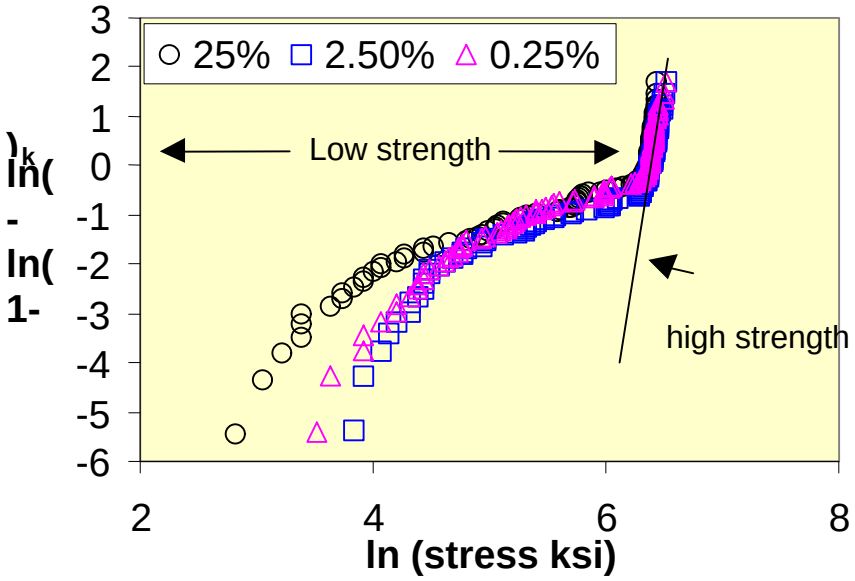

Figure 30 Weibull Plot for Strength of 1996 Vintage Cable from Several Cable Reels

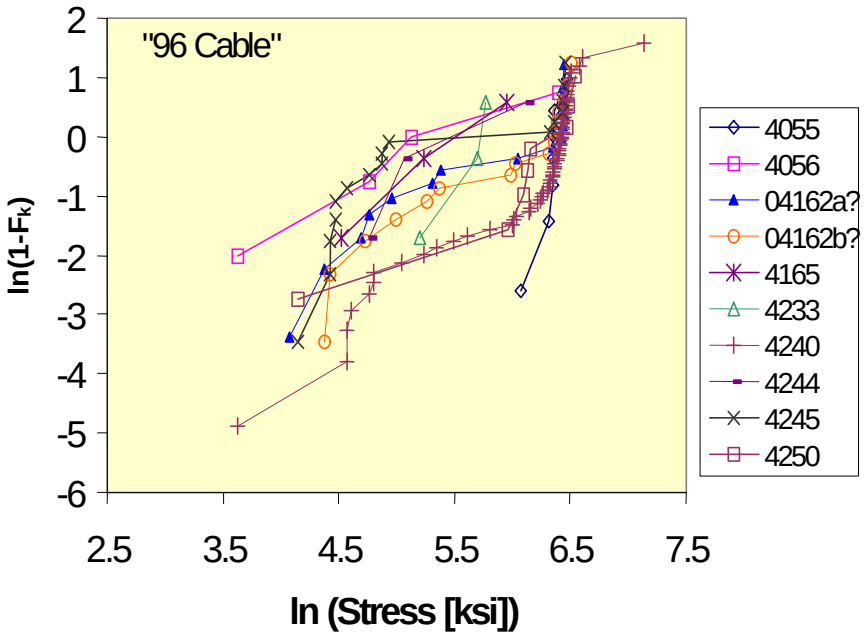

Figure 31 Strength Data for 1996 Cable by Strain Rate

7.2 Strength Testing of Fiber Throughout Cabling and Including HF Exposure

The results of the initial testing showed that more than one type of defect is affecting the strength of the cabled fiber. A second round of strength testing was performed to look at each of the cabling process steps' affect on the cabled fiber strength. The significant process steps studied were: respooling, buffering, strength member application and jacketing. After each of these steps, the fiber was strength tested and samples were exposed to HF vapor. Table 9 shows the test approach.

Table 9 Second Strength Test Approach

				Remaining Sample Lengths at End of Test/Operation (meters)					
Seq. #	**Operation or Test**	**Length Used**	**Test Location**	**CDO384XB (Control)**	**CDO384XC (HF)**	**CDO384XE (Strength)**	**CDO588XB (HF)**	**CDO588XC (Strength)**	**CDO588XD (Control)**
	Starting Sample Lengths	(m)		1870	489	483	518	809	935
1	Visible Fault Location			1870	489	483	518	809	935
2	Initial Dynamic Tensile Strength Tests			1847	460	459	504	787	918
3	OTDR (850nm??)		BHB	1847	460	459	504	787	918
4	Loss (1300nm)		BHB	1847	460	459	504	787	918
5	Retain Individual Control Sample	50	BHB		410	409	454	737	
6	Remove HF Etch Samples	10	BHB		400		444		
7	Remove Dynamic Tensile Samples	30	BHB			379		707	
8	Dynamic Tensile Strength		BHB						
9	HF Exposure/Visual Exam		GSFC						
10	Respool/Laser Mike Exam		BICC		400	379	444	707	
11	Visible Fault Location		BICC		400	379	444	707	
12	Remove Dynamic Tensile Samples	30	BICC			349		677	
13	Remove HF Etch Samples	10	BICC		390		434		
14	Dynamic Tensile Strength		BHB						
15	HF Exposure/Visual Exam		GSFC						
16	Extrude FEP Loose Tube Buffer	40	BICC		350	309	394	637	
17	Visible Fault Location (respool?)		BICC		350	309	394	637	
18	Remove Dynamic Tensile Samples	30	BICC			279		607	
19	Remove HF Etch Samples	10	BICC		340		384		
20	Dynamic Tensile Strength		BHB						
21	HF Exposure/Visual Exam		GSFC						
22	Apply Strength Member		BICC		340	279	384	607	

Table 9 Second Strength Test Approach (Cont'd)

				Remaining Sample Lengths at End of Test/Operation (meters)					
Seq. #	**Operation or Test**	**Length Used**	**Test Location**	**CDO384XB (Control)**	**CDO384XC (HF)**	**CDO384XE (Strength)**	**CDO588XB (HF)**	**CDO588XC (Strength)**	**CDO588XD (Control)**
23	Visible Fault Location (respool?)		BICC		340	279	384	607	
26	Dynamic Tensile Strength		BHB						
29	Visible Fault Location (respool?)		BICC		290	209	334	537	
30	Remove Dynamic Tensile Samples	30	BICC			179		507	
31	Remove HF Etch Samples	10	BICC		280		324		
32	Dynamic Tensile Strength		BHB						
33	HF Exposure/Visual Exam		GSFC						

[ref-21]

7.2.1 Results: Strength Testing of Fiber Throughout Cabling and Including HF Exposure

The results of the second round of strength testing are shown in Figures 32a through 32d. [ref-22, 23, 24] Figures 33a through 33d show the endfaces of the fibers at the low strength breaks.

a.

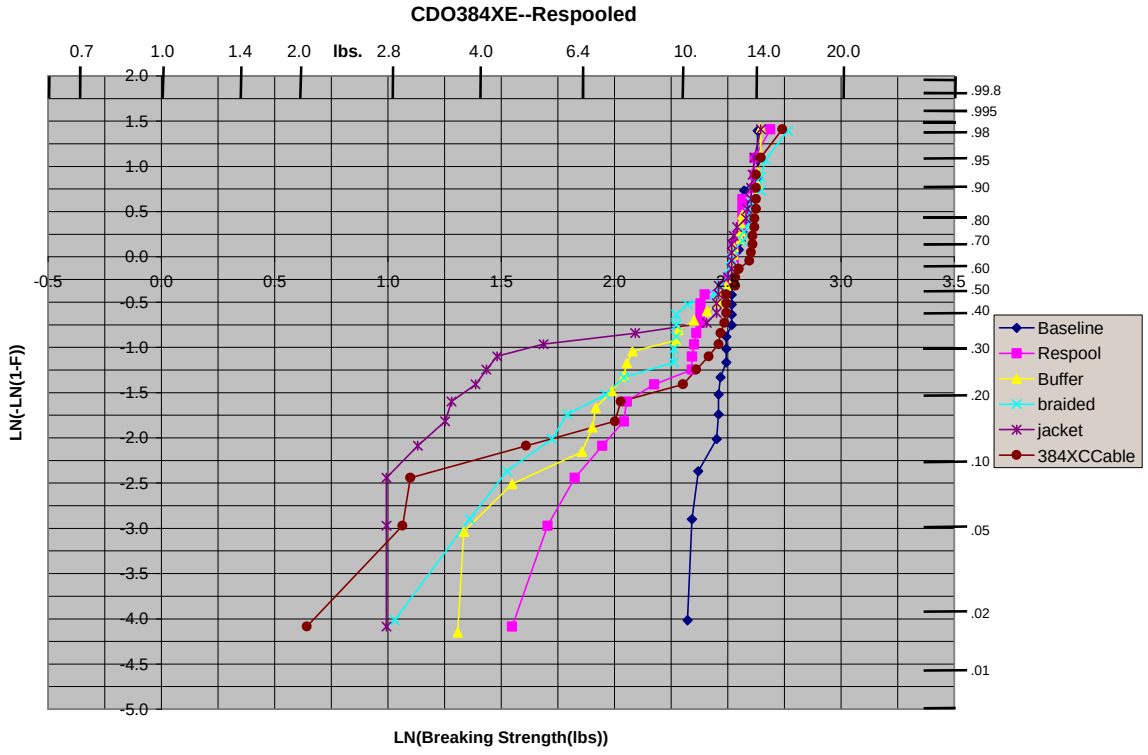

b.

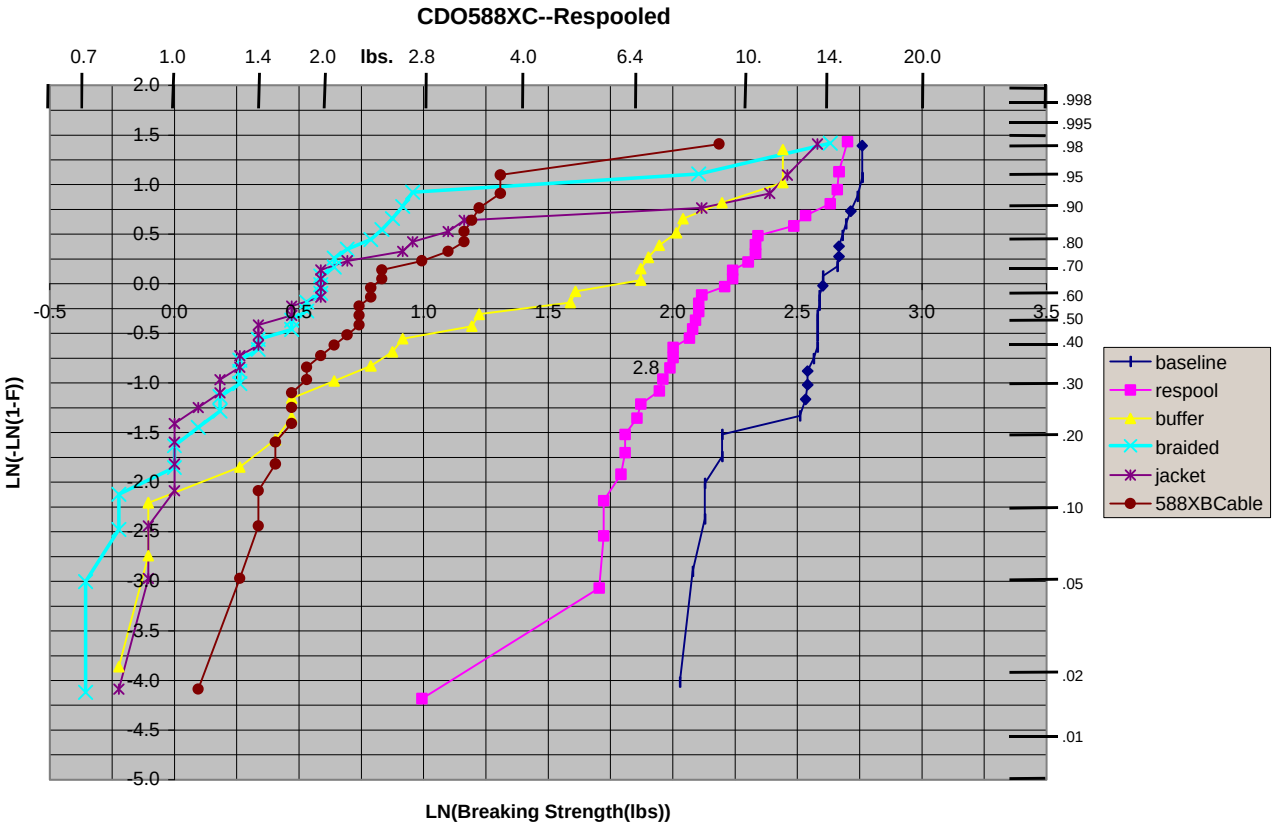
CDO588XC--Respooled
0.7
1.0
1.4
2.0
lbs.
2.8
4.0
6.4
10.
14.
20.0
2.0
1.5
1.0
0.5
0.0
-0.5
-1.0
-1.5
-2.0
-2.5
-3.0
-3.5
-4.0
-4.5
-5.0
-0.5
0.0
0.5
1.0
1.5
2.0
2.5
3.0
3.5
2.8
.998
.995
.98
.95
.90
.80
.70
.60
.50
.40
.30
.20
.10
.05
.02
.01
LN(-LN(1-F))
LN(Breaking Strength(lbs))
baseline
respool
buffer
braided
jacket
588XBCable